*Transactions* of the SMiRT 27
Yokohama, Japan, March 3-8, 2024
Division II

# EXPERIMENTAL AND THEORITICAL APPROACH OF FUEL RUPTURE. GAZ BUBBLES STABILITY

**Gatt Jean-Marie, Hela Mensi, Zachari-Aubrun Isabelle, Michel Bruno,**

Research Scientist, CEA, DES, IRESNE, DEC, France, jean-marie.gatt@cea.fr

## ABSTRACT

In the context of the fuel rupture ($UO_2$), a study of gas bubbles stability is proposed. These bubbles are created during irradiation. For that, a cohesive zone approach is used. The proposed model depends on two parameters, the critical stress and the critical energy release rate. That latter parameter presents a material property and could be easily measurable thanks to notched micro-cantilevers bending tests, prepared in fresh and irradiated $UO_2$ fuel (Figure 2). Nevertheless, the critical stress is more complicated to define. Indeed, this parameter measure the stress concentration due the presence of local defects (porosity, gas bubbles …), ii) the cantilever shape (embedding), or the presence of grain boundary. In addition, this parameter is not experimentally directly accessible.
The fresh $UO_2$ samples (without grain boundary) broke, as expected, at the cantilever base, where the stresses are the highest. However, for the samples presenting large defects or grain boundaries the crack generated follows those latter.
Based on these experimental data and the cohesive zone approach, the main goal is to study the pressurized intra-granular bubble stability at various zones of the fuel pellet.

## INTRODUCTION

In the context of the fuel rupture, we propose to study the stability of gas bubbles, which are created during irradiation. For that, a cohesive zone approach [1] [2] [3] [4] [5] [6] is used. The proposed model depends on two parameters, the critical stress and the critical energy release rate. These parameters can be identified tanks to bending tests on notched micro-cantilevers, prepared in fresh and irradiated $UO_2$ fuel [12]. A molecular dynamic approach can be also used [7] [8] [10]. Nevertheless, the critical stress is more complicated to define. Indeed, this parameter should describe the stress concentration due to the presence of local defects (porosity, gas bubbles …), the cantilever shape (embedding), and the presence or not of grain boundary. In addition, this parameter is not experimentally accessible.
The fresh and irradiated $UO_2$ samples [12] (without grain boundary) broke, as expected, at the cantilever base, where the stresses are the highest. However, for the samples presenting large defects or grain boundaries the crack generated follows those latter.
Based on these experimental data and the cohesive zone approach, the main goal is to study the pressurized bubble stability at various zones of the fuel: intra-granular zones.

## MATERIALS PROPERIES

To evaluate the fracture properties, fracture stress and fracture energy (from toughness measurement), two approaches are proposed:

- Experimental approach using bending tests at the grain scale
- Numerical approach using molecular dynamic

For experimental approach, we use bending tests as show in Figure 1:

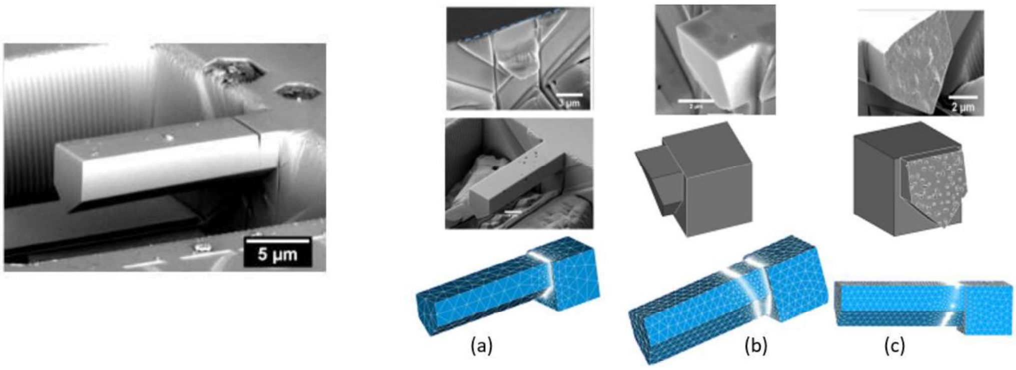


Figure 1. Experimental tests and simulations associated

This experimental approach is associated to numerical simulations to interpret the tests. The toughness is measured using notched beam. However, for rupture stress, it is more difficult. Indeed, we do not know exactly where the crack initiates. To obtain the rupture stress we choose to use dynamic molecular approach.

The atomic potential used is the CRG potential (Cooper-Rushton-Grimes) for UO2 [7]. It is composed of three potentials: Buckingham potential [7] for gas, Morse potential [8] witch acts at short distances and Coulomb potential witch take into account the long-distance interactions. We also use an N-bodies potential acting at short range: EAM potential. The elastic coefficient are first calculated to test the potential. The Table 1 show a good correspondence between the experimental measurements and those calculated in dynamic molecular.

Table 1: Elastic Coefficient for UO2

| | $C_{11}$ (GPa) | $C_{11}$ (GPa) | $C_{11}$ (GPa) |
|---|---|---|---|
| Exp [12] | 396 | 121 | 64 |
| CRG [7] | 406 | 125 | 64 |

From these data, the critical stress and energy obtain by dynamic molecular; it is possible to evaluate the stability of gas bubbles present in the fuel.

## BUBLES POPULATIONS

In the fuel, we can observe different bubbles populations:

- Intra-granular
- Inter-granular
- Precipitation
- HBS

These bubbles have different complex forms and internal pressure. In this article, only intra-granular bubbles are taken into account with a geometrical description based on a spherical shape.

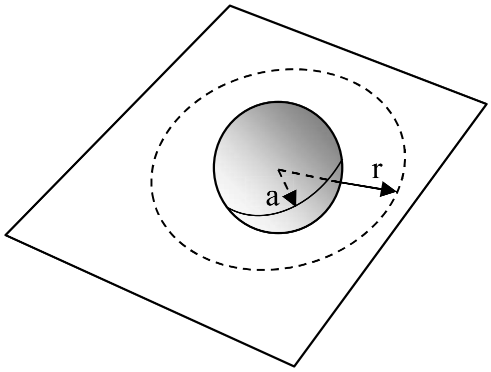


Figure 2. Spherical bubble (radius “a”) with its rupture plan

We consider a pressurized spherical bubble, of radius “a”, in an elastic ceramic matrix (Figure 2). The pressure seen by the matrix will be noted: $\wp$. This pressure is worth [9]:

$$\wp = P - \frac{2\gamma}{a} = P - \frac{G_c}{a} \quad (1)$$

γ is the surface tension, which is equal to $G_c/2$, with $G_c$ the Griffith energy and P the gas pressure inside the bubble.

***Gas bubbles stability analysis***

The balance equation is:

$$\frac{\partial \sigma_{rr}}{\partial r} + \frac{1}{r}(\sigma_{rr} - \sigma_{\theta\theta}) = 0 \quad with\ \sigma_{\theta\theta} = \sigma_{\varphi\varphi} \qquad (2)$$

We put $x = \frac{r}{a} \geq 1$ and $\mu = \frac{E}{2(1+\upsilon)}$, the compatibility equations and elastic behavior law:

$$\begin{cases} \varepsilon_r = \frac{\partial u_r}{\partial r} \\ \varepsilon_\theta = \frac{u_r}{r} \\ \varepsilon_z = \frac{\partial u_z}{\partial z} \end{cases} \Rightarrow \frac{\partial}{\partial r}(r\varepsilon_\theta) = \varepsilon_r \ \text{ and } \begin{cases} \varepsilon_r = \frac{\sigma_r}{E} - \frac{\nu}{E}\sigma_\theta \\ \varepsilon_\theta = \frac{\sigma_\theta}{E} - \frac{\nu}{E}\sigma_r \\ \varepsilon_z = -\frac{\nu}{E}(\sigma_r + \sigma_\theta) \end{cases} \qquad (3)$$

The stresses and strains fields written:

$$\begin{cases} \sigma_r = -\frac{\wp}{x^3} \\ \sigma_\theta = \sigma_\varphi = \frac{\wp}{2x^3} \end{cases} \quad \text{and} \quad \begin{cases} \varepsilon_r = -\frac{1}{2\mu}\frac{\wp}{x^3} \\ \varepsilon_\theta = \varepsilon_\varphi = \frac{1}{4\mu}\frac{\wp}{x^3} \end{cases} \qquad (4)$$

From equation (3) and (4), the stored elastic energy can be deduced:

$$E_{el} = \int_V \frac{1}{2}\left(\sigma_r.\varepsilon_r + \sigma_\theta.\varepsilon_\theta + \sigma_\varphi.\varepsilon_\varphi\right)dV \qquad (5)$$

Then:

$$E_{el} = \frac{\pi a^3}{2\mu} \wp^2 \left(1 - \frac{1}{x^3}\right) \tag{6}$$

Furthermore, the energy required to create a crack with surface S is:

$$\mathrm{E_f} = \mathrm{G}_c\mathrm{S} = \pi \mathrm{G}_c a^2(x^2 - 1) \tag{7}$$

There is crack initiation if the two criteria, energy and stress are verified.
This leads to verify that:

$$\begin{cases} E_{el}(x) \geq \pi \mathrm{G}_c a^2(x^2-1) \\ \sigma_\theta(x)\big(= \sigma_\varphi(x)\big) \geq \sigma_c \end{cases} \tag{8}$$

We obtain the two following equations:

$$\frac{\pi a^3}{2\mu} \wp^2 \left(1 - \frac{1}{x^3}\right) \geq \pi \mathrm{G}_c a^2(x^2-1) \;\; and \;\; \frac{1}{2}\wp\left(\frac{a}{r}\right)^3 = \frac{\wp}{2x^3} \geq \sigma_c \tag{9}$$

This can be expressed as:

$$\wp \geq \sqrt{\frac{2\mu \mathrm{G}_c}{a}\left(\frac{x^3(x+1)}{x^2+x+1}\right)} \;\text{ et }\; \wp \geq 2\sigma_c x^3 \tag{10}$$

We put: $K_{en} = \sqrt{\frac{4\mu G_c}{3a}}$ and $K_{co} = 2\sigma_c$.

The two parameters, $K_{en}$ and $K_{co}$, are associated respectively with the energy criterion and the stress criterion. These two constants have the dimension of a stress, that is to say joules per unit of volume (J/m$^3$). The crack initiation condition is that the two criteria are verified at x=1:

$$\wp \geq K_{en} \;\text{ and }\; \wp \geq K_{co}$$

From this two equations a stability criteria can be deduced. The bubble is stable if:

$$\wp < K_{enmin} \;\; or \;\; \wp < K_{comin}$$

$K_{enmin}$ *and* $K_{comin}$ are the minimal values deduced from material properties

In order to better understand crack propagation, the criterion can be evaluated according to available material properties, for x>1. To do this, two functions associated with the two criteria must be introduced.

- The function $g(x) = K_{co}x^3$. This function, linked to stress criterion, is strictly increasing with $g(1) = K_{co}$. This function $g$, which have a simple behavior, is used as reference.
- The function$f(x) = K_{en}\sqrt{\frac{x^3(x+1)}{x^2+x+1}}$. This function, linked to energy criterion, can be written as :

$$f(x) = K_{en}x\sqrt{\frac{1}{1+\frac{1}{x(x+1)}}} \qquad f(1) = K_{en}\sqrt{\frac{2}{3}} \tag{11}$$

For x much greater than one, we have: $f(x) = K_{en}x$, so a linear evolution (asymptotic behavior). We define:

$$\mathcal{K} = \left(\frac{K_{en}}{K_{co}}\right)^2 \tag{12}$$

Three cases must be considered:

In the first case**:** $\mathcal{K} = \frac{\mathbf{3}}{\mathbf{2}}$

$$g(x) = K_{co}x^3 \;\; and \;\; g(1) = K_{en}\sqrt{\frac{2}{3}} = K_c$$

$$f(x) > 0, g(x) > 0 \;\; and \;\; f(1) = g(1)$$

We put:

$$f(x) = g(x) \Rightarrow f^2(x) = g^2(x) \Leftrightarrow K_{en}^2 = \frac{(x+1)}{(x^2+x+1)} = K_{co}^2 x^3$$

and

$$\begin{cases} H(x) = x^5 + x^4 + x^3 - K(x+1) \\ H'(x) = 5x^4 + 4x^3 + 3x^2 - K \\ H''(x) = 20x^3 + 12x^2 + 6x > 0 \end{cases}$$

The function $H'$ is increasing and $H'(1) = 12 - K > 0$
The function $H$ is then strictly increasing with $H(1) = 0$. We find:

$$f(1) = g(1) = K_{en}\sqrt{\frac{2}{3}} = K_{co}$$

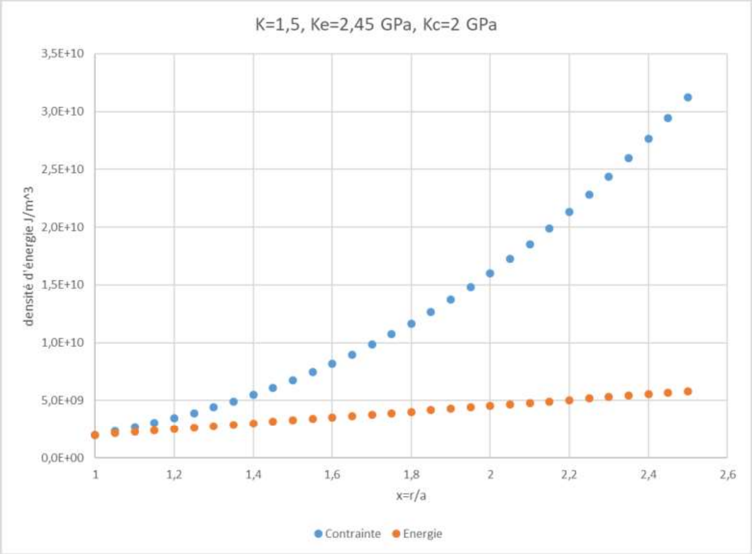


Figure 2: Energy density evolution with the ratio x/a in the case where $\mathcal{K}$ =1.5

The Figure 2 shows that the stress and energy criteria are verify simultaneously at x=1. This lead to the start of the crack (or much localized damage). In this case, there is rupture without propagation of the crack. This is a very particular solution, which does not really make physical sense.

**In the second case: $\mathcal{K} > \frac{3}{2}$**

$$f(1) = K_{en}\sqrt{\frac{2}{3}} > K_{co} = g(1)$$

$$g(x) = K_{co}x^3 \;\; et \;\; g(1) = K_{co} < K_{en}\sqrt{\frac{2}{3}}$$

$$f(x) = K_{en}\sqrt{\frac{x^3(x+1)}{(x^2+x+1)}} \;\; et \;\; f(1) = K_{en}\sqrt{\frac{2}{3}} > K_{co}$$

There are two points of intersection between the two curves if: $\exists x > 1/g(x) = f(x)$. Therefore, we have:

$$H(x) = x^5 + x^4 + x^3 - K(x+1) = 0 \;\; and \;\; H(1) = 3 - 2K < 0$$
$$H'(x) = 5x^4 + 4x^3 + 3x^2 - K$$
$$H''(x) = 20x^3 + 12x^2 + 6x > 0$$

The $H'$ function is therefore increasing and we have:

$$H'(1) = 12 - K \text{ and } H(1) = 3 - 2K < 0$$

Two cases can existed:

- $K \geq 12$ $=> H'(1) \leq 0 \Rightarrow$ H is a decreasing and then increasing function
- $1{,}5 < K < 12$ $=> H'(x) > 0 \Rightarrow$ H is an increasing function

$H$ is increasing when x tend to infinity with $H(1) = 3 - 2K < 0$, therefore exists a point such as : $H(x) = 0$ :

$$K_e \frac{(x+1)}{(x^2+x+1)} = x^3$$
$$\frac{K_c}{x^3} = 1 + \frac{x^2}{(x+1)}$$

In this case, we have a continuous, decreasing and positive function $(\frac{K}{x^3})$ and an increasing and positive function $(1 + \frac{x^2}{x+1})$. So there is one intersection point between the two curves as showed Figure 3.

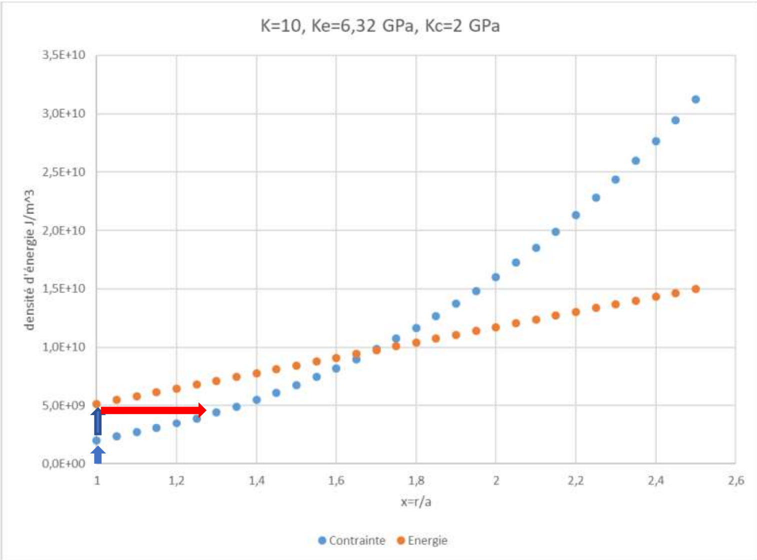


Figure 3: $\boldsymbol{\mathcal{K}} > 1.5$: Stable propagation (at the start)

On the figure 2 above, the stress criterion is reached first (blue curve). The pressure in the bubble must continue to increase until it reaches the energy criterion (orange curve). At this moment, the rupture appears and propagates (red arrow). In this case, we obtain "stable" crack propagation.

- In the third case : $\mathcal{K} < \frac{3}{2}$ :

$$f(1) = K_e\sqrt{\frac{2}{3}} < K_c = g(1), \text{ i.e : } \boldsymbol{\mathcal{K}} < \frac{3}{2}$$

$$H(x) = x^5 + x^4 + x^3 - K(x+1) = 0$$

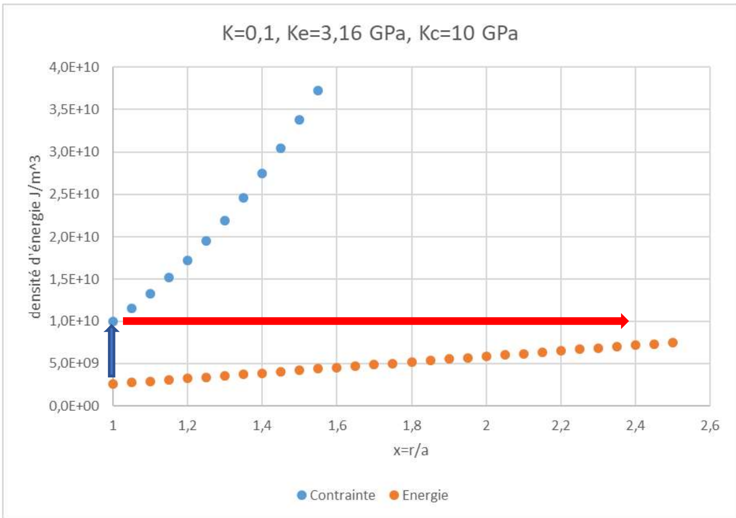


Figure 4: $\mathcal{K}$ **< 1.5**: Dynamic propagation

In the figure 4, the energy criterion is first verified. The pressure in the bubble continue to increase (blue arrow) until it reaches the stress criterion, which implies a sudden rupture of the bubble (red arrow).
In summarize, function of $\mathcal{K}$, which is defined as the square of the ration between the energy criteria ($K_{en}$) and stress criteria ($K_{co}$): $\mathcal{K} = \left(\frac{K_{en}}{K_{co}}\right)^2$, there are principally two rupture mechanisms:

- For $\mathcal{K}$ **<3/2**: The energy criterion is first verified at the surface of the bubble. The pressure must therefore continue to increase to reach the stress criterion. Meanwhile, the energy in the bubble continues to grow. The crack appears to release the important stored energy. The propagation of the crack is, in this case, unstable.

- Pour $\mathcal{K}$ **>3/2**: The constraint criterion is checked first. The pressure in the bubble must continue to increase to reach the energy criterion. Once reached, a crack appears, dissipating the stored energy. The crack therefore tends to stop quickly. In this case, the propagation is described as stable.

In summary, depending on the value of $\mathcal{K}$, which is defined as the square of the ratio between the energy criterion ($K_{en}$) and the stress criterion ($K_{co}$): $\mathcal{K} = \left(\frac{K_{en}}{K_{co}}\right)^2$, there are mainly two break mechanisms:

For $\mathcal{K}$ <3/2: The energy criterion is first checked at the surface of the bubble. The pressure must therefore continue to increase to reach the stress criterion. Meanwhile, the energy in the bubble continues to grow. The crack appears to release the important stored energy. The propagation of the crack is, in this case, unstable.

For $\mathcal{K}$ >3/2: The stress criterion is first checked. The pressure in the bubble must continue to increase to reach the energy criterion. Once this criterion reached, a crack appears, dissipating the stored energy. The crack therefore tends to stop quickly. In this case, the propagation is stable.
In our case, according to Table 5, we have K<1.5, the unstable regime is activated if the rupture criteria are reached. This is generally not the case for nano-metric bubbles.

## STABILITY STUDY OF INTRAGRANULAR BUBBLES

The data are provided by Margaret [13]. This code gives the evolution of gaseous fission products with gaz concentration, number and size of bubbles in the fuel (formation, and pressure evolution) during irradiation in the reactor and the storage. The bubbles are stables if :

$$\frac{\wp}{K_{enmin}} < 1 \;\; or \;\; \frac{\wp}{K_{comin}} < 1$$

Depending of the results given §2, the parameters $K_{en}$ and $K_{co}$ can be framed (Tableau 1) by minimum and maximum values.

| Kcomin (GPa) | Kcomax (GPa) | Kenmin (GPa) | Kenmax (GPa) |
|---|---|---|---|
| 14 | 20 | 6.73 | 48.4 |

*Tableau 1 : Ko and Ken for each intra-granular phases*

The stability criterion can now be checked using the results issus of Margaret code. We find the results presented in Figure 5 below:

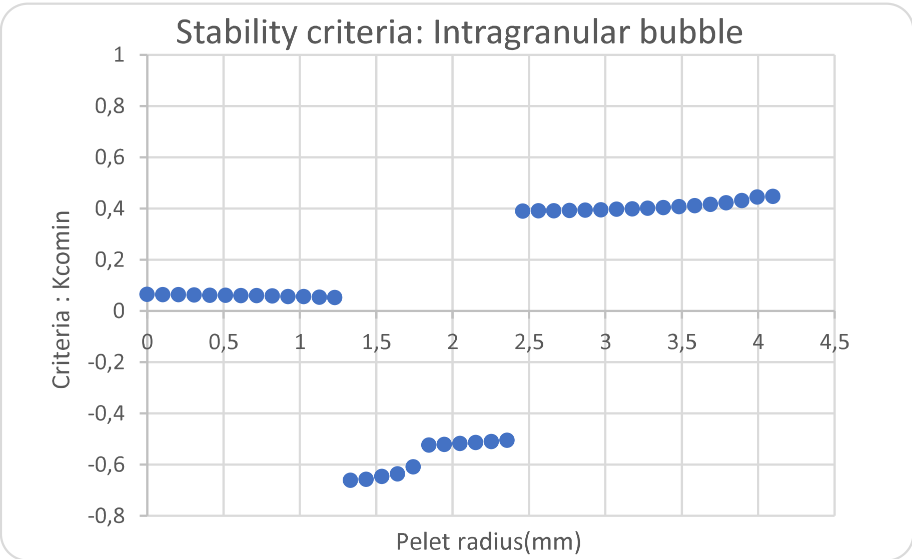


*Figure 5: verification of criteria for intra-granular bubbles*

## CONCLUSION

The inter-granular bubbles population has been studies. We showed this population stays stable during storage of the fuel. The others populations (intergranulaires and HBS) have not been studies. In fact, to studies these last bubbles populations, we need more data on grain boundary properties.

## REFERENCES

[1] B. Michel and all, State of the art of fuel micro-mechanical modelling: From atomic scale to engineering laws in fuel performance codes, JNM 572, 2022

[2] D. Leguillon, Strenght or toughness? A criterion for crack onset at a notch, Eur. J. of Mechanic A, 20

[3] D. Leguillon, D. Quesada, C. Putot, E. Martin, Prediction of crack initiation at blunt notch and cavities-size effect, Eng. Frac. Mech, Vol 74, No 15

[4] E. Martin, T. Vandellos, D. Leguillon, N. Carrère

[5] A. Doitran, P. Cornetti, A. Sapora, R. Estevez, Experimental and theoretical characterization of mixed mode brittle failure from square hole, Inter. Journal of fracture

[6] A. Doitrand, E. Martin, and D. Leguillon, “Numerical implementation of the coupled criterion: Matched asymptotic and full finite element approaches,” *Finite Elem. Anal. Des.*, vol. 168, p. 103344, 2020.

[7] M.W.D. Cooper, H.J.D. Rushton, R.W. Grimes, A many body potential approach to modelling the thermomechanical properties of actinide oxide, J. Phy. Coden. Matter, Vol 26, 10, 2014.

[8] Morse P. M., “Diatomic Molecules According to the Wave Mechanics. II. Vibrational Levels,” *Phys. Rev.*, vol. 34, pp. 57–64, 1929.

[9] A.A. Griffith, The phenomena of rupture and flow in solids”, Philosophical Transactions of the Royal Society of London, A, vol 221, pp 163-198, 1920

[10] S.D. Daw, Muray, M. Foiles, Stephen, I. Baskes. The embedded-atom method: a rewiew of theory and application; Mate. Sci. Report, Vol.9, Sept 1992 pp 251-310, 1993

[11] H. Balboa, L. Van Brutzel, A. Chartier, and Y. Le Bouar, “Assessment of empirical potential for MOX nuclear fuels and thermomechanical properties,” *J. Nucl. Mater.*, vol. 495, 2017.

[12] I. Zacharie-Aubrun *et al.*, “Effects of irradiation on mechanical properties of nuclear UO2 fuels evaluated by Vickers indentation at room temperature,” *J. Nucl. Mater.*, vol. 547, 2021

[13] L. Noirot, MARGARET: A comprehensive code for the description of fission gas behaviour, Nuclear Engineering and Design, 241, 2011.